different and those of the latter are more shifted to higher j values. That is, diatomic photofragments get more rotational angular momentum by the action of the torque of the anisotropy of the intermolecular potential as they depart from other fragment.

We can see from Table 7 that the resonance width in the molecular parameters chosen is around 2×10^{-6} eV and about ten times smaller than the value of rotational constant, 16.2×10^{-6} eV. That is, the resonance life time is more than ten times larger than the rotational period. It may be considered that resonance states live long enough to forget the ground state information. The fact that IOS approximation holds well means that the decomposition takes place much faster than the rotation of the diatomic fragment. This derives from the fact that the kinetic energy of the relative motion of photofragments is thousand times larger than the rotational energy.

Acknowledgment. This work was supported by KOSEF under Contract No. 913-0303-001-2.

References

1. Beneventi, L.; Casavecchia, P.; Volpi, G. G.; Bieler, C. R.; Janda, K. C. *J. Chem. Phys.* **1993**, *98*, 178 and references therein.
2. Schinke, R.; Engel, V. *Faraday Discuss. Chem. Soc.* **1986**, *82*, paper 11.
3. (a) Miller, W. H. *Adv. Chem. Phys.* **1975**, *25*, 69. (b) *ibid* **1975**, *30*, 77.
4. Fano, U.; Rau, A. R. P. *Atomic Collisions and Spectra*; Academic: Orlando, 1986.
5. Lee, C. W. *Bull. Korean Chem. Soc.* **1991**, *12*, 228.
6. Greene, C. H.; Rau, A. R. P.; Fano, U. *Phys. Rev.* **1982**, *A26*, 2441.
7. (a) See reference 2. (b) Buckingham, A. D.; Fowler, P. W.; Hutson, J. M. *Chem. Rev.* **1988**, *88*, 963.
8. Halberstadt, N.; Beswick, J. A.; Janda, K. C. *J. Chem. Phys.* **1987**, *87*, 3966.
9. Child, M. S. *Molecular Collision Theory*; Academic: London, 1974.
10. Lester, W. *Methods. Comput. Phys.* **1971**, *10*, 243.
11. Hager, W. W. *Applied Numerical Linear Algebra*; Prentice-Hall International: London, 1988.
12. Janda, K. C. *Adv. Chem. Phys.* **1985**, *20*, 201.
13. (a) McGuire, P. *Chem. Phys. Lett.* **1973**, *23*, 575. (b) Mcguire, P.; Kouri, D. J. *J. Chem. Phys.* **1974**, *60*, 2488. (c) Pack, R. T. *J. Chem. Phys.* **1974**, *60*, 633. (d) Schinke, R. *J. Phys. Chem.* **1986**, *90*, 1742.
14. Taylor, J. R. *Scattering Theory*; John Wiley and Sons: New York, 1972.
15. Smith, F. T. *J. Chem. Phys.* **1962**, *36*, 248.
16. Lee, C. W. *Bull. Korean. Chem. Soc.* **1995**, *20*, 850.

Assignment of the Redox Potentials of Cytochrome c_3 of *Desulfovibrio vulgaris* Hildenborough by ^{1}H NMR

Jang-Su Park*, Shin Won Kang, and Jung-Hyu Shin†

Department of chemistry, College of Natural Sciences, Pusan National University, Pusan 609-735, Korea
†Department of Chemistry, Seoul National University, Seoul 151-742, Korea
Received July 3, 1995

The heme assignment of the ^{1}H NMR spectrum of cytochrome c_3 of *Desulfovibrio vulgaris* Hildenborough within the X-ray structure were fully cross established according to their redox potential. The major reduction of the heme turned out to take place in the order of hemes IV, I, II and III (the heme numbers indicating the order of bonding to the primary sequence). This assignment can provide the physicochemical basis for the elucidation of electron transfer of this protein.

Introduction

Cytochrome c_3 are a family of low molecular weight (13 kDa) electron-transfer protein that may be isolated from sulfate-reducing bacteria.[1,2] The proteins contain 4 hemes in a single polypeptide and show very low redox potentials.[3] Cytochrome c_3 are electron carriers required for the electron transfer between hydrogenases[4] and smaller carriers. *In vitro*, they facilitate the electron transfer from hydrogenase to flavodoxin and rubredoxin[5] and are a necessary component of several different redox reaction in crude extracts.

*To whom correspondances should be addressed.

Crystal structures of cytochrome c_3 from *Desulfovibrio desulfuricans* Norway (*Dd*N), *Desulfovibrio vulgaris* Miyazaki F (*Dv*MF) and *Desulfovibrio vulgaris* Hildenborough (*Dv*H).[6~9] The two proteins are closely homologous. The redox potential of cytochrome c_3 is an important parameter in understanding its physiological role. Macroscopic and microscopic redox potentials were determined for a series of cytochrome c_3.[10~13] The assignment for *Dv*MF cytochrome c_3 of the microscopic redox potentials to the hemes in the crystal structure has been performed by means of NMR.[14] A correlation between the microscopic redox potentials and the crystal structure has been reported for cytochrome c_3 from *Dd*N.[15] It is interesting to compar the redox processes of two cy-

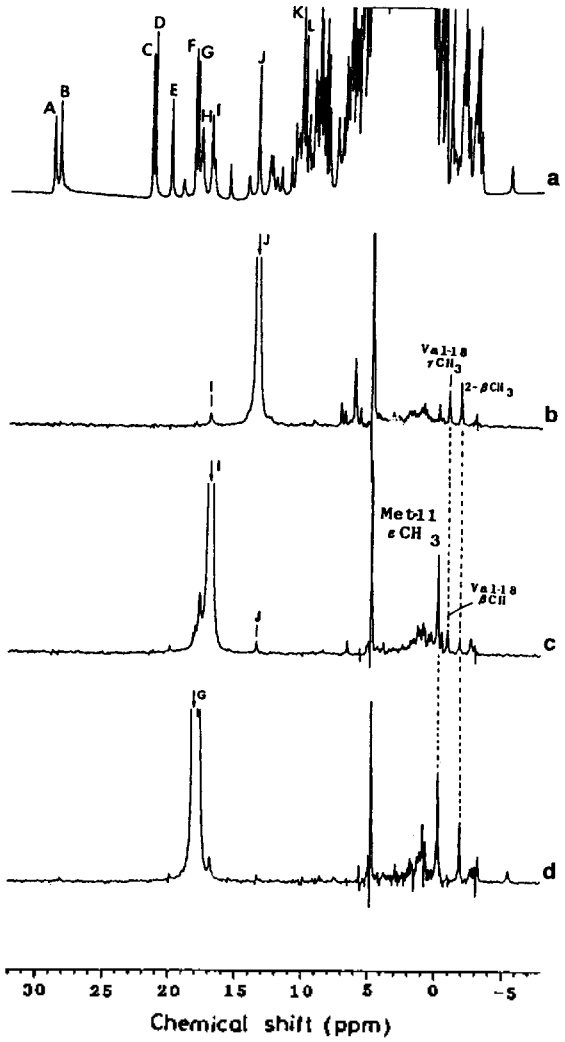

Figure 1. 400 MHz ^{1}H NMR spectra of ferricytochrome c_3 from *D. vulgaris* Hildenborough in 30 mM phosphate buffer (p^2H 7.0) at 30 ℃. The methyl signals are labeled alphabetically. (a) A normal spectrum. (b-d) NOE difference spectra. The allows indicate the irradiated positions. The signal at 4.73 ppm comes from H^2HO. The assignment of the signals is given in the text.

tochrome c_3 from two different strains, *Dv*MF and *Dv*H. Especially, the understanding of the influence of their structural differences on the interheme interaction is of importance. In this paper we reported ^{1}H NMR study, through 1D NOE measurements and 2D techniques, of the Hildenborough protein and proposed assignments of heme redox potentials. The result agreed with the assignment by Salgueiro *et al.*[16] Formore, our assignment facilitates the use of NMR to both monitor the interaction of cytochrome c_3 with biological redox partners and analyze the orientation and dynamics of residues defining the heme pocket.

Materials and Methods

Desulfovibrio vulgaris Hildenborough was cultured in medium C.[3] Cytochrome c_3 was purified according to the reported procedure.[17] The purity index (A552(red)/A280(ox)) of the

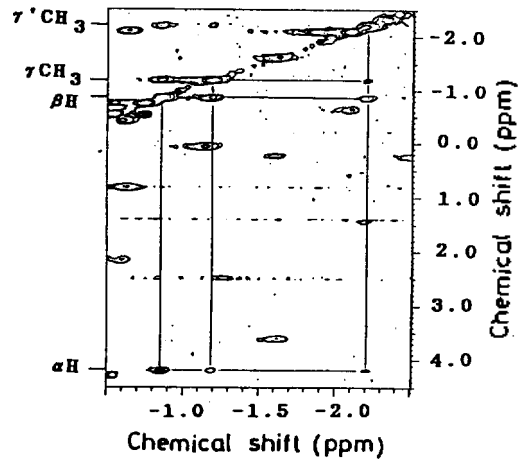

Figure 2. A section of two-dimensional TOCSY (HOHAHA) spectrum of ferricytochrome c_3 at 30 ℃, showing the J-connectivities for the side-chain spin system of valine residue, which was assigned to Val-18 (see text).

final sample was over 3.0. The purity was also confirmed by SDS-polyacrylamide gel electrophoresis. 400 MHz ^{1}H NMR spectra of 2.0 mM cytochrome c_3 in 30 mM phosphate buffer (p^2H 7.0) were measured at 30 ℃ with a Bruker AM-400 NMR spectrometer. Chemical shifts are presented in parts per million relative to the internal standard 2,2-dimethyl-2-silapentane-5-sulfonate (DSS). The nuclear Overhauser effect (NOE) experiments were performed with 0.5 s pre-irradiation and the accumulation of 4800 transients. The differece spectrum was obtained by subtracting the on-resonance free induction decay (FID) from the off-resonance FID. 2D TOCSY (HOHAHA) spectra were measured at 30 ℃ with the data size of 512×2048, spectral width of 8064 Hz and mixing time of 26.6 ms. 2D-COSY spectra were measured at 30 ℃ and 50 ℃ with the data size of 512×2048 and spectral width of 13900 Hz. The p^2H values reported in this paper are pH-meter readings uncorrected for isotop effects.

Results and Discussion

A 400 MHz ^{1}H NMR spectrum of ferricytochrome c_3 is shown at the top of Figure 1.

As reported earlier,[13] eleven heme methyl signals can be observed separately in the downfield region. They are labeled alphabetically from the downfield. They were classified to four hemes on the basis of the electron distribution probabilities in the five macroscopic oxidation states,[13] namely,

heme 1; A, H, I and K,
heme 2; B, F and G,
heme 3; C and G,
heme 4; E and J,

where hemes were numbered according to the order of the major reduction.

NOE measurement was carried out in the NMR experiment. NOE difference spectra with irradiation of heme methyl proton at signals I, J and G are presented in Figure 1b-d. On irradiation of proton at signal I, NOE was observed at signal J (Figure 1c) and vice versa (Figure 1b). Because there is no overlapping at signals I and J, and because they

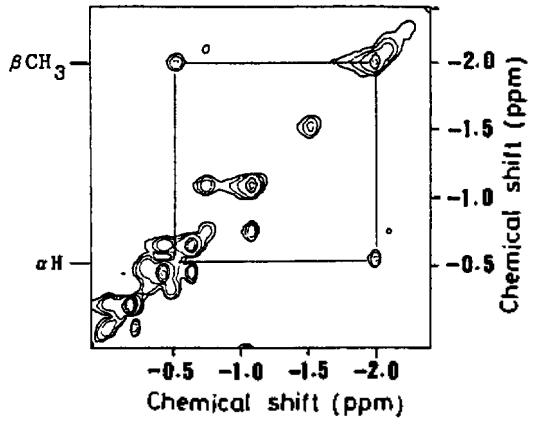

Figure 3. Section of TOCSY (HOHAHA) spectrum of ferricytochrome c_3 at 30 ℃, showing the J-connectivities for the heme side chain in the thioether bridge.

belong to heme 1 and heme 4, respectively, we can conclude that this is the interheme NOE. The crystal structure of this protein shows that the shortest interheme methyl carbon distance is 4.0 Å (methyl 5 of heme IV-methyl 1 of heme III; Roman numbers indicating the order of bonding to the primary sequence). Furthermore, the NOE signal commonly observed at −0.98 ppm in Figure 1b and c was assigned to the γ-methyl protons of valine residue on the basis of the connectivities in 2D-DQFCOSY and TOCSY spectra. The latter is presented in Figure 2.

In the crystal structure, the carbon of γ-CH_3 of Val-18 is located in the distances of 4.3 and 3.7 Å from 5-CH_3 of heme IV and 1-CH_3 of heme III, respectively. No other shorter distance was found for between carbons of γ-CH_3 of valine and heme IV and heme methyl groups. Accordingly, the common NOE signal at −0.98 ppm in Figure 1b and c can be assigned to γ-CH_3 of Val-18. A strong NOE was also observed at −0.28 ppm on irradiation at signal I (Figure 1c). The same NOE signal appeared on irradiation at signal G (Figure 1d). This signal showed three-proton intensity. In a 2D-TOCSY and COSY spectra, this signal has no cross peak, suggesting that this is an isolated methyl proton spins. Therefore, it is εCH$_3$ of methionine. The chemical shift of this signal is unusually high in comparison with that of a normal methionine. This is consistent with the close proximity of this methyl grop to porphyrin rings. In the crystal structure, only the εCH$_3$ of Met-11 was found to be close to heme methyl groups. It is located at a distance of 4.1 Å and 3.9 Å from the 5-CH_3 of heme IV and the 5-CH_3 of heme I, respectively, in terms of carbon distance. Therefore, signal I and G can be assigned to the 5-CH_3 of hemes IV and I.

On irradiation at signal J, a strong NOE was observed at −1.98 ppm (Figure 1b). The same NOE signal appeared on irradiation at signals I and G (Figure 1c and d). The signal has a three-proton intensity. The relevent part of TOCSY spectrum is presented in Figure 3.

This chemical group should have A_3X_n spin as a part of its coupled spin system. Such a spin system can be attributed to either alanine or heme side chain in the thioether bridge. Since the cross peak of this spin system in the TOCSY spectrum disappeared with a longer mixing time (74.7 ms), this

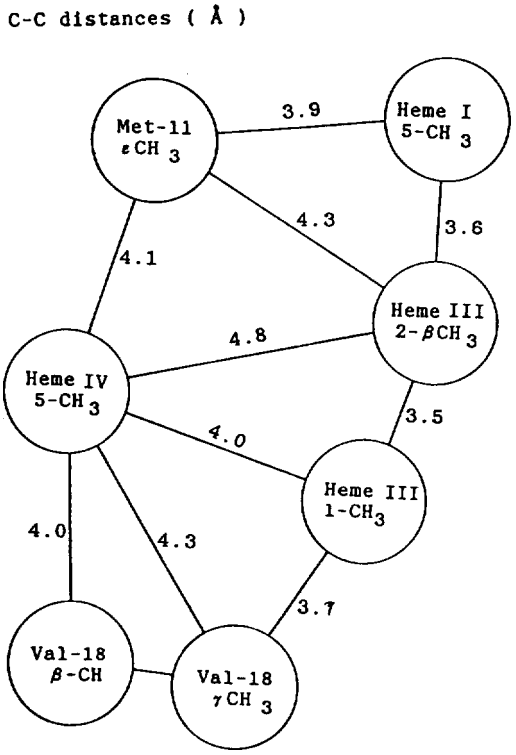

Figure 4. Correlation between the NOE network (solid lines) and the intercarbon distances (Å) in the crystal structure. The assignment is given in the text.

can be assigned to the heme side chain, namely, βCH$_3$ in the thioether bridge. The β-methyl group in the vicinity of 5-CH_3 of hemes I and IV in the crystal structure was 2-βCH$_3$ of heme III. Their carbon distances were 3.6 Å and 4.8 Å, respectively. Comparing the intensity of the NOE signals in Figure 1, signals I and G can be attributed to 5-CH_3 of hemes IV and I, respectively. Signal J can be assigned to 1-CH_3 of heme III. This assignment was supported by the NOE among the signal I, J and side chain of Val-18 as shown in Figure 1b and c.

The NOE network and the corresponding carbon distances in crystal structure were summarized in Figure 4.

The excellent matching in Figure 4 confirms the reliability of the assignment and suggests that the crystal structure is maintained in solution to a great extent.

Signal I, G and J belong to the hemes mainly reduced at the first, second and fourth reduction steps, respectively. Therefore, it can be concluded that hemes IV, I, II and III in the crystal structure are mainly reduced in this order. In other words, they can be assigned to hemes 1, 2, 3 and 4 (numbering due to the order of major reduction), respectively.[13] This assignment agreed with earlier results by Salgueira *et al.*.[16] On the basis of this assignment, the microscopic redox potentials established by Park *et al.*[13] now can be attributed to the individual hemes in the crystal structure. Thus, this complete assignment enables us to investigate the structural factors which determine the redox potential of each heme in a tetraheme protein. For example, A cooperative interheme interaction was shown for the pair of hemes 2 and 3 by Park *et al.*.[13] This pair can be attributed to hemes

I and II in the crystal structure on basis of our assignment. Their interiron distance is 11.2 Å and is the shortest in this protein. Furthermore, Phe-20, which is conserved in most cytochrome c_3 so far sequenced, is heme I and imidazole ring ligated to heme II. The cooperative interheme interaction would be connected with this specific conformation. However, this is the subject for future investigation.

Conclusions

Although the X-ray structure of cytochrome c_3 from *Dv*H has been obtain[8,9] its coordinates are not yet available and so those of cytochrome c_3 from *Dv*MF[7] were used for the assignment of reduction state.[18] The two proteins are closely homologous, as is the relative architecture of their four hemes, which is also maintained in the much less homologous protein *Dd*N.[19] Furthermore, comparison of 1D-NMR spectra of cytochrome c_3 from *Dv*MF[14] and *Dv*H shows that the redox patterns are quite similar, though not identical, as indeed are the heme methyl group shifts for the fully oxidised state.

There may be small differences in the relative redox potentials of four hemes in the *Dv*MF and *Dv*H proteins, but the overall pattern appears to be the same. However, a different order of redox potentials has been proposed for the much less homologous cytochrome c_3 from *Dd*N on the basis of single crystal EPR studies.[15] Such a diffeence would reflect the influence of the polypeptide chain. Studies to elucidate the physicochemical and physiological significance of the control of redox potentials are currently in progress.

Acknowledgment. This work was supported by the Basic Science Research Institute, Ministry of Education, Korea (BSRI-94-3410 and BSRI-94-7402). The authors are grateful to prof. H. Akutsu, Yokohama National University for his assistance.

References

1. Legall, J.; Moure, J. J. G.; Peck, H. D.; Xavier, A. V. *Iron-Sulfur Proteins*; Spiro, T. G. (ed.), Wiley, New York 1982, p 177.
2. Yagio, T.; Inokuchi, H.; Kimura, K. *Acc. Chem. Res.* **1983**, *16*, 2.
3. Postgate, J. R. *The sulfate-Reduciog Bacteria*; 2nd edn., Cambridge University Press: Cambridge 1984.
4. LeGall, J.; Fauque, G. *Biology of Anaerobic Microorganisms*; Zehnder, A. J. B., ed., John Wiley and Sons: New York, 1988, p 587.
5. Bell, G. R.; Lee, J. P.; Peck, H. D., Jr.; LeGall, J. *Biochemie* **1978**, *60*, 315.
6. Pierrot, M.; Haser, R.; Frey, M.; Payan, F.; Astier, J. P. *J. Biol. Chem.* **1982**, *257*, 14341.
7. Higuchi, Y.; Kusunoki, M.; Matsuura, Y.; Yasuoka, N.; Kakudo, M. *J. Mol. Biol.* **1984**, *172*, 109.
8. Morimoto, Y.; Tani, T.; Okumura, H.; Higuchi, Y.; Yasuoka, N. *J. Biochem. (Tokyo)* **1991**, *110*, 532.
9. Matias, P. M.; Frazao, C.; Morais, J.; Coll, M.; Carrondo, M. A. *J. Mol. Biol.* **1993**, *234*, 680.
10. Bruschi, M.; Loutfi, M.; Bianco, P.; Haladjian, J. *Biochem. Biophys. Res. Commun.* **1984**, *120*, 384.
11. Niki, K.; Kawasaki, Y.; Higuchi, Y.; Yasuoka, N. *Langmuir* **1987**, *3*, 982.
12. Fan, K.; Akutsu, H.; Kyogoku, Y.; Niki, K. *Biochemistry* **1990**, *29*, 2257.
13. Park, J.-S.; Kang, S.; Choi, S. *Bull. Korean Chem. Soc.* **1995**, *16*, 331.
14. Park, J.-S.; Kano, K.; Niki, K.; Akutsu, H. *FEBS* **1991**, *285*, 149.
15. Guigliarelli, B.; Bertrand, P.; Moore, C.; Haser, R.; Gayad, J. P. *J. Mol. Biol.* **1990**, *216*, 161.
16. Salgueiro, C. A.; Turner, D. L.; Santos, H.; LeGall, J.; Xavier, A. *FEBS* **1992**, *314*, 155.
17. Park, J.-S.; Enoki, M.; Ohbu, A.; Fan, K.; Kyogoku, Y.; Niki, K.; Akutsu, H. *J. Mol. Struct.* **1991**, *242*, 343.
18. Turner, D. L.; Salgueiro, C. A.; LeGall, J.; Xavier, A. *Eur. J. Biochem.* **1992**, *210*, 931.
19. Coutinho, I. B.; Turner, D. L.; LeGall, J.; Xavier, A. V. *Eur. J. Biochem.* **1992**, *209*, 329.